Article

Tantalum Oxide Thin Films Sputter-Deposited by Oxygen Gas Pulsing

Nicolas Martin [1,*], Jean-Marc Cote [1], Joseph Gavoille [1] and Valérie Potin [2]

[1] Institut FEMTO-ST, SUPMICROTECH-ENSMM, CNRS, 15B, Avenue des Montboucons, CEDEX, 25030 Besancon, France; jeanmarc.cote@femto-st.fr (J.-M.C.); joseph.gavoille@ens2m.fr (J.G.)
[2] Laboratoire Interdisciplinaire Carnot de Bourgogne (ICB), UMR 6303, CNRS, Univ. Bourgogne Franche-Comté, 9, Avenue Alain Savary, BP 47 870, CEDEX, F-21078 Dijon, France; valerie.potin@u-bourgogne.fr
* Correspondence: nicolas.martin@femto-st.fr; Tel.: +33-363-08-2431

Abstract: Tantalum oxide thin films are deposited by DC reactive magnetron sputtering from a tantalum metallic target and argon + oxygen. The oxygen gas is pulsed during the deposition with a constant pulsing period T = 10 s, whereas the introduction time of the reactive gas, namely the t_{ON} injection time, is systematically changed from 0 to 100 % of T. Therefore, composition of as-deposited TaO_x films is continuously changed from pure metallic tantalum to the over-stoichiometric Ta_2O_5 material. Films adopt the body-centered cubic structure (metallic Ta) for the lowest t_{ON} injection time values (oxygen stoichiometry $x < 1.0$) and become amorphous for the longest ones. It is shown that the t_{ON} injection time is a key parameter to deposit either homogeneous tantalum oxides, or periodic Ta/TaO_x multilayers with alternations close to 3 nm. Optical transmittance in the visible region of the film/glass substrate system and electrical conductivity vs. temperature both exhibit a gradual evolution from metallic ($\sigma_{300K} = 8.17 \times 10^5$ S m^{-1} with an opaque behavior) to semiconducting ($\sigma_{300K} = 1.97 \times 10^3$ S m^{-1} with a semi-transparent transmittance) and finally to dielectric properties ($\sigma_{300K} < 10^{-5}$ S m^{-1} for interferential films) as a function of the oxygen concentration in the films.

Keywords: tantalum oxide; thin film; reactive sputtering; gas pulsing; metal; semiconductor; dielectric; periodic multilayers

1. Introduction

Over the past few decades, many investigations have been focused on the growth and fabrication of thin films based on transition metal oxides [1,2]. These materials are particularly attractive for their great potential in electronic, magnetic, and optical applications. They have been studied and sometimes integrated into various devices such as gas sensors [3], electrochromic systems [4] and catalysts [5], among others. Film behaviors are strongly influenced by the structure at the micro- and nanoscale, but they primarily depend on their chemical composition, especially the oxygen content. As a result, playing with the metalloid concentration in metal oxide thin films appears as an attractive strategy for tuning many physico-chemical properties [6–8]. While some transition metal oxides have been deeply investigated due to a spontaneous formation or a quite convenient way to prepare them, some metal oxides like tantalum oxides [9,10] have been less studied and their deposition as a thin solid film with tunable compositions still remains a challenging task.

Tantalum oxide compounds exhibit a great technological interest, particularly because of their optical and electrical performances [11–13]. This kind of materials has attracted huge attention these last years due to some potential applications as high refractive index compounds in high-finesses mirrors [14], anti-reflecting coatings for solar cells [15], optical waveguides [16], or dielectric capacitors in high-density dynamic random-access

memories (DRAMs) [17–19]. Compared to silicon dioxide material, which exhibits a dielectric constant of 3.9, stoichiometric tantalum pentoxide Ta_2O_5 compound can produce about 5 to 6 times more capacitance density (dielectric constant of Ta_2O_5 is in between 20 and 27). This can provide a high packing density in the next generations of DRAMs without reducing the thickness of dielectric materials down to unachievable values. Because of such a technological attraction, tantalum oxide thin films have been grown by a large variety of deposition methods including anodization, room temperature oxidation, ion-assisted deposition, chemical vapor deposition (CVD) and physical vapor deposition (PVD) [20–25]. TaO_x films prepared by these different techniques showed widely dispersed properties depending on the process parameters, temperature grown, post-annealing conditions, etc. However, the influence of the oxygen concentration on some characteristics of as-deposited films has insufficiently been investigated, especially for films prepared by reactive sputtering [26]. It mainly comes from some difficulties to synthesize metal oxide compounds and so Ta-based thin films, with tunable element concentrations, due to instabilities of the reactive sputtering process [27–29]. This drawback reduces the range of reachable chemical compositions and consequently the resulting properties.

The purpose of this paper is to show how a pulsing injection of the oxygen gas can extend the range of oxygen contents and thus the resulting properties of sputter-deposited TaO_x films. The role of the pulsing parameters (injection time of the oxygen gas into the deposition process, namely the t_{ON} injection time in the remaining parts of the article) on the film properties is principally investigated. A systematic increase in this oxygen injection time leads to amorphous tantalum oxides corresponding to a vanishing of the columnar structure, and for the shortest t_{ON} injection times, the growth of periodic and nanometric multilayers are clearly prepared. Optical characteristics in the visible region show that TaO_x films sputter-deposited with short t_{ON} injection times are mainly absorbent, whereas a high oxygen supply tends to produce semi-transparent and interferential Ta_2O_5 compounds. The reverse evolution of oxygen and tantalum concentrations is observed vs. the t_{ON} injection time, and correlates with the evolution of the film electrical properties where a smooth transition of properties is obtained starting from metallic-like for films with the lowest oxygen contents to insulating-like behaviors for oxygen-rich films.

2. Materials and Methods

Deposition of tantalum oxide thin films was performed by dc reactive magnetron sputtering inside a 40 L stainless-steel vacuum reactor. The latter was equipped with a circular planar and water-cooled magnetron sputtering source. It was evacuated with a turbomolecular pump backed by a mechanical pump to obtain a residual pressure of 10^{-6} Pa. The pumping speed was kept constant at S = 13 L s^{-1}. The tantalum target (purity 99.6 at. %, 50 mm diameter) was DC-sputtered with a constant current density J_{Ta} = 51 A m^{-2} in a reactive atmosphere composed of argon and oxygen gases. Argon flow rate was maintained at 4.4 sccm corresponding to an argon partial pressure of 0.3 Pa. A homemade computer-controlled system, namely the Reactive Gas Pulsing Process—RGPP, was used to introduce oxygen flow rate vs. time according to a rectangular shape [30]. A constant pulsing period T = 10 s was applied. A maximum oxygen flow rate q_{O2Max} = 1.6 sccm was used whereas the minimum oxygen flow rate was fixed at q_{O2min}= 0 sccm. Then, t_{ON} and t_{OFF} times were inversely and systematically changed from t_{ON} = 0 to 10 s. Tuning only the t_{ON} injection time (and consequently the t_{OFF} time) is a simple approach to manage the reactive gas introduction into the sputtering process. As a result, playing with this single operating parameter leads to tune the oxygen concentration in the films (to see later in Section 3.1) and thus, it allows adjusting physical properties of tantalum oxide thin films. The target-to-substrate distance was 65 mm. Glass and (100) silicon wafer substrates were introduced through a 1 L airlock. Before each run, they were cleaned with acetone and alcohol, and the tantalum target was pre-sputtered in a pure argon atmosphere for five minutes before introducing oxygen, in order to remove the target surface contamination layer. Room temperature was used for all samples and the deposition time was adjusted in order to obtain

a film thickness close to 500 nm (measured by a mechanical profilometer after the deposition stage). The chemical composition of the films deposited on (100) silicon wafer was determined by electron probe microanalysis (EPMA). Observations of the film's cross-section were performed by scanning electron microscopy (SEM). Optical transmittance spectra of tantalum oxide coatings deposited on glass substrates were recorded from a Lambda 20 UV–visible Perkin-Elmer spectrophotometer. The crystallographic structure was investigated by X-ray diffraction (XRD) using monochromatic Co K_{α} radiation with a θ/2θ configuration. Electrical conductivity was measured vs. temperature using the van der Pauw method in a temperature range from 293 to 543 K. Microstructural analysis was carried out with a JEOL JEM 2100 LaB_6 Transmission Electron Microscope (TEM) operating at 200 keV. Cross-sections for TEM were prepared using the standard sandwich technique. They were mechanically polished, dimpled down to a thickness of 10 μm and Ar^+ ion milled to electron transparency. The TEM images were analyzed using the GATAN Digital Micrograph software. Chemical composition was also measured with a better spatial resolution by energy-dispersive X-ray spectroscopy implemented in the TEM (JEOL 2300 EDT).

3. Results and Discussion

3.1. Composition and Structure

Deposition rate of TaO_x films is first determined as a function of the t_{ON} injection time from the film's thickness measured by a mechanical profilometer (500 nm as a target) and knowing the deposition time (Figure 1).

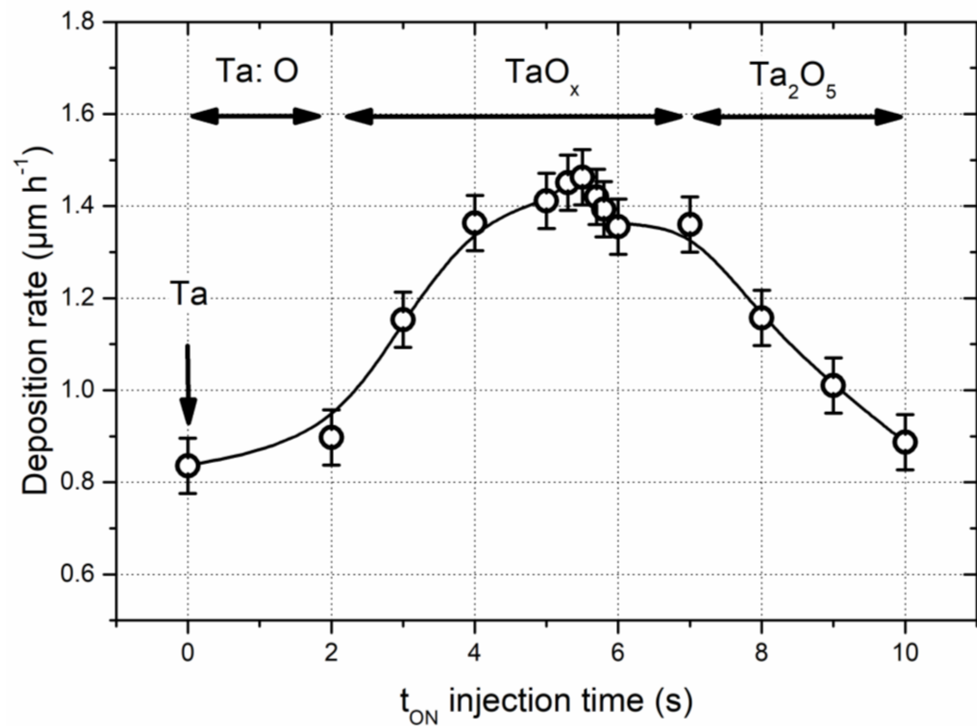

Figure 1. Influence of t_{ON} injection time on the TaO_x deposition rate. Oxygen mass flow rate is pulsed with a constant rectangular period T = 10 s. Deposition rate gradually changes and exhibits a maximum for t_{ON} close to 5 s. Three zones, namely Ta:O, TaO_x, and Ta_2O_5-like compounds, are suggested as a function of the t_{ON} injection time.

No abrupt drops of the deposition rate are obtained for a given supply of the oxygen gas, as commonly observed for transition metal oxide thin films sputter-deposited by the conventional reactive sputtering process (injection of a constant mass flow rate) [31]. A smooth and continuous evolution is rather produced when increasing the t_{ON} injection time. Without oxygen, pure metallic Ta films are prepared with a deposition rate of 0.84

μm h^{-1}. Injecting the oxygen gas with t_{ON} injection times of a few seconds leads to a significant increase in the deposition rate. The latter reaches a maximum value of 1.46 μm h^{-1} in-between t_{ON} = 4–6 s. This order of magnitude of pulsing period T and t_{ON} injection time (i.e., a few seconds) is related to the kinetics of poisoning and cleaning mechanisms of the metallic target surface by reactive gases like oxygen or nitrogen, as typically reported in reactive sputtering processes [32].

A further increase in the t_{ON} injection time reduces the rate. The latter reduces down to 0.9 μm h^{-1} for a constant supply of oxygen mass flow rate (i.e., t_{ON} = 10 s). This continuous variation of deposition rate vs. t_{ON} injection time with an optimized condition is often obtained for oxides and nitrides prepared by reactive sputtering implementing RGPP [33]. However, most of these ceramic thin films (e.g., TiO_2, ZrO_2, V_2O_5 …) exhibit a much lower deposition rate than that of the corresponding metal when the metallic target completely works in the poisoned sputtering mode (t_{ON} injection time tending to the pulsing period T). A few-nanometer-thick compound layer (oxide for reactive sputtering with O_2, and nitride with N_2) is formed on the target surface with a low sputtering yield, which reduces the deposition rate compared to that of pure metal. For reactive sputtering of tantalum oxides (and also similarly reported for tungsten oxides [34]), rates corresponding to the deposition of the most stable and nearly stoichiometric compound (i.e., Ta_2O_5 in this study) is high or close to the same order of magnitude as the metallic one. Based on former investigations proposed by Oechsner et al., Ta_2O_5 is a particular compound since its sputtering yield can be higher than that of the clean metal [35]. According to the same authors, this unusual behavior of Ta_2O_5 (also expected for tungsten and niobium oxides) gives rise to the sputtering of TaO and Ta neutral species as well as ionic, neutral and molecular oxygen. It is worth of noting that this high deposition rate of tantalum oxides is also connected to a balance between sputtering yield, kinetics of poisoning of the target surface, oxygen concentration and density of the deposited oxide, as previously reported for WO_x thin films [34].

Assuming the t_{ON} injection time as a key parameter for producing TaO_x films with various compositions, one may suggest three zones in Figure 1. Two zones correspond to the deposition of Ta:O films for the very short t_{ON} injection times (lower than about 2 s), and amorphous a-Ta_2O_5-like films for the longest ones (higher than about 6 s). Between these two t_{ON} injection times, TaO_x compounds can be prepared. These adjustable film compositions are well illustrated, plotting the tantalum and oxygen concentrations as a function of the t_{ON} injection time (Figure 2).

Both concentrations exhibit a continuous and gradual variation as t_{ON} rises. From the shortest t_{ON} injection time of 1 s, the oxygen content reaches 7 at. % and increases rapidly up to 47% for t_{ON} = 3 s. A reverse evolution is clearly measured for the tantalum content with a symmetric drop of its concentration as the t_{ON} injection time changes. Nearly equivalent Ta and O concentrations are obtained when t_{ON} is around 3 s. Afterwards, and for t_{ON} injection times higher than 4 s, tantalum oxide films become oxygen-rich and both concentrations tend to stabilize to values corresponding to the stoichiometric Ta_2O_5 compound (dashed lines in Figure 2). It is also worth of remarking that over-stoichiometric tantalum oxide thin films are prepared for t_{ON} injection times higher than 6 s and tending to a constant supply of oxygen. These oxygen-rich metal oxide compounds are often produced when the reactive sputtering process is fully set in the poisoned mode. These operating conditions give rise to the formation of an oxide layer on the target surface, which is sputtered in an argon + oxygen atmosphere. As-deposited films are then all over-oxidized.

This symmetric, reverse and smooth evolution of metal and metalloid concentrations vs. t_{ON} injection time has never been reported for other metal oxide thin films sputter-deposited by RGPP playing only with the injection time of the oxygen gas [36]. As t_{ON} increases, metal oxide (MeO_x) films become oxygen-rich, while the metal concentration symmetrically decreases. This correlates with an alternation of the sputtering mode between the metallic and oxidation one. These results chiefly prove and illustrate that RGPP is a valuable approach to precisely tune the chemical composition of MeO_x films (from sub- to over-stoichiometric oxide compounds). This issue can be quite difficult to reach by

conventional reactive sputtering (due to non-linear phenomena), and without implementing some feedback control systems or high pumping speed of the deposition chamber [37–39].

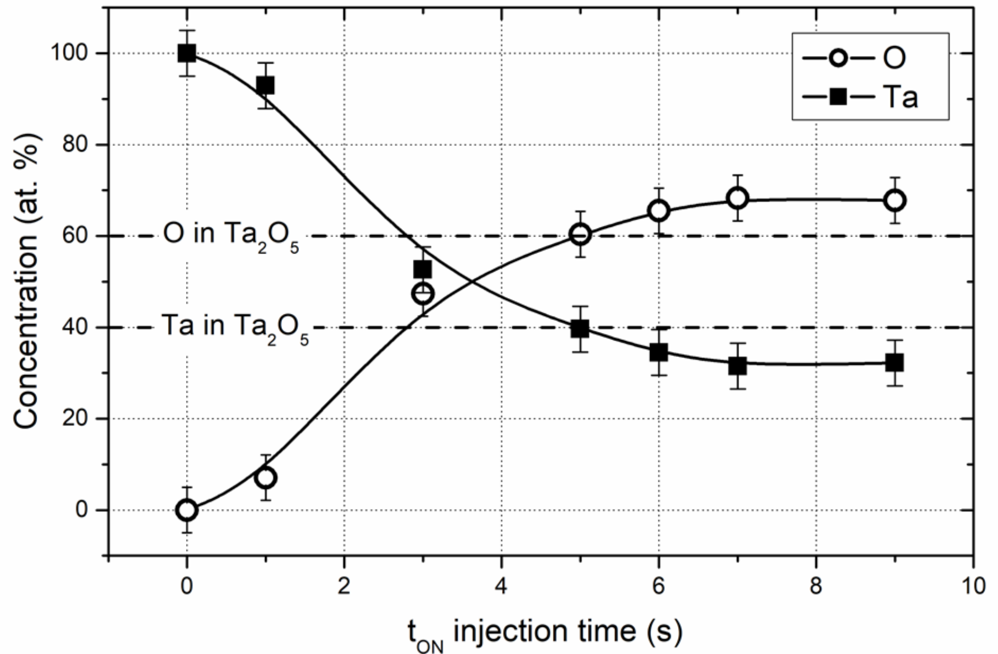

Figure 2. Tantalum and oxygen atomic concentrations as a function of the t_{ON} injection time. A continuous and reverse evolution is measured for both elements as t_{ON} increases. Solid lines are a guide for the eye. Horizontal dashed lines correspond to oxygen and tantalum concentrations of the stoichiometric Ta_2O_5 compound.

X-ray diffraction analyses of TaO_x films show that the crystalline structure is also influenced by the oxygen pulsing, particularly for t_{ON} injection times lower than 6 s (Figure 3). Without oxygen supply and as expected (not shown here), the typical pattern of a pure Ta film is obtained with diffracted signals corresponding to the bcc (body-centered cubic) α-phase. The shortest injection time of the oxygen gas (t_{ON} = 1 s) gives rise to weak and broad diffracted signals. Most of them are related to the α-Ta ground state bcc structure with a crystal size of a few nanometers. It is interesting to note the occurrence of two significant peaks at 2θ = 34.80° and 64.51° assigned to (002) and (413) planes of the β-Ta metastable tetragonal structure, respectively. This metastable β-Ta phase has ever been reported for the deposition of Ta films by sputtering, particularly when impurities like residual oxygen are present during the deposition process [35,40–42]. These results can also be compared to the binary phase diagram of the Ta-O system [43]. The latter shows the co-existence of α- and β-phases for a wide range of concentrations (from 1 to 71 at. % of oxygen) and the occurrence of the β-phase for an oxygen concentration lower than 1 at. % at room temperature.

Colin et al. [44] pertinently showed that some mechanisms (stress, deposited energy per atom) occurring during the early growth stages of Ta deposition favor the preferential nucleation of the β-Ta phase and its stabilization over the film thickness. They also demonstrated the key role of interface layer formation on the crystalline phase occurrence, with a major role of an amorphous Ta interlayer. For our tantalum oxide films prepared by RGPP with the shortest t_{ON} injection times, the t_{OFF} time is long enough to mainly keep the process in the elemental sputtering mode. As a result, a t_{ON} injection time of 1 s periodically supplies oxygen to prevent the growth of the most stable α-Ta phase leading to an amorphization of the deposited film, and favoring the formation of the β-Ta phase. For these operating conditions, both α- and β-Ta phases coexist, and longer pulsing periods would promote the formation of the α-Ta phase [44].

Increasing further the t_{ON} injection time to 3 s induces even more the growth of an amorphous structure. Two broad signals around 35° and 65° are clearly recorded by XRD. They correspond to the range of 2θ angles related to α- and β-Ta phases, more accurately defined for t_{ON} = 1 s. This longer t_{ON} injection time prevents the process to remain mainly in the elemental sputtering mode. It rather extends it in the oxidized sputtering mode and an alternation between these two modes is then established. The long-range order of the α- or β-Ta phase cannot be obtained to produce clear diffracted signals and an amorphous structure prevails. For t_{ON} injection times higher than 5 s, amorphization of the films is still more noticeable. The broad signal close to 2θ = 35° is shifted to lower angles and corresponds neither to the α- nor to the β-Ta phase. For films prepared with t_{ON} injection times higher than 6 s, XRD does not exhibit any diffracted signal, but the same broad envelop, with 2θ = 20–40°, and a weaker one close to 2θ = 55°. This type of patterns is typical of tantalum oxide thin films sputter-deposited at room temperature. These results well agree with former investigations previously published by others [45,46]. They are indicative of an amorphous structure of as-deposited Ta_2O_5 films on unheated substrates [47], or a possible nano-crystalline structure with sub-nanometric grains assigned to the orthorhombic phase of tantalum pentoxide compound [26].

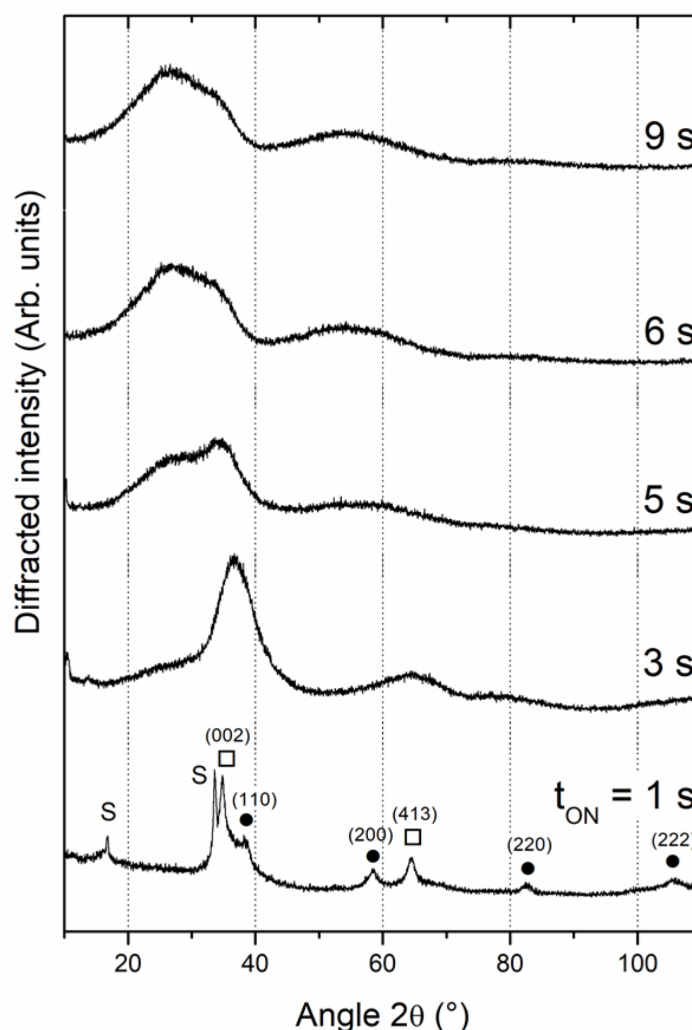

Figure 3. X-ray diffraction patterns of TaO_x thin films prepared with various t_{ON} injection times. S = silicon substrate; ● = α-Ta ground state bcc structure; □ = β-Ta metastable tetragonal structure.

Chittinan et al. also deposited tantalum oxide films by reactive sputtering with the same strategy, i.e., oxygen pulsing [48]. In the same way, they produced films exhibiting

an amorphous structure by conventional reactive sputtering or whatever their pulsing conditions. They recorded very similar X-ray diffraction patterns to our results obtained with t_{ON} injection times higher than 5 s, as shown in Figure 3.

Cross-section observations by scanning electron microscopy (SEM) show a poorly defined microstructure of tantalum oxide films sputter-deposited with various t_{ON} injection times (Figure 4). The typical columnar architecture of pure Ta films (not shown here) becomes less distinct even for the lowest t_{ON} of 1 s (Figure 4a). A brittle behavior is rather produced for films deposited with injection times lower than 6 s, where some fractures of the silicon wafer are extended from the substrate through the film thickness. This also means that tantalum oxide films present signs of a quite good adhesion to the silicon, despite the oxygen pulsing and deposition with no external heating of the substrate.

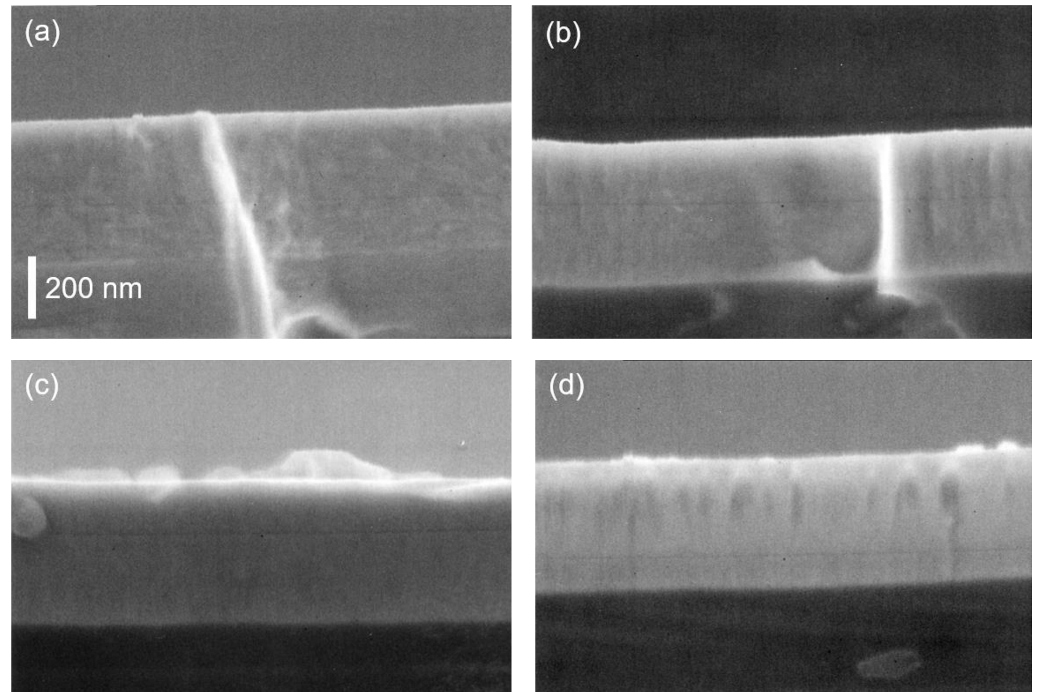

Figure 4. Cross-section pictures by SEM of tantalum oxide thin films sputter-deposited on Si substrates for different t_{ON} injection times: (**a**) t_{ON} = 1 s, (**b**) t_{ON} = 5 s, (**c**) t_{ON} = 6 s, (**d**) t_{ON} = 9 s. The scale bar is the same for all SEM pictures.

For the longest t_{ON} injection times (e.g., t_{ON} = 9 s), a columnar growth becomes more distinguishable (Figure 4d). These pulsing conditions correspond to a nearly constant supply of the oxygen gas (reactive sputtering process mainly in oxidized mode). From composition analyses (Figure 2), the deposition of tantalum oxide films tends to the stoichiometric Ta_2O_5 compound. This cross-section microstructure agrees with observations performed by Ito et al., who sputter-deposited tantalum pentoxide films at room temperature [49]. The authors similarly noticed a columnar structure corresponding to the first zone of structural zone models for films prepared at room temperature with a density lower than that of the bulk Ta_2O_5 [50].

The poorly defined microstructure observed from SEM cross-sections (Figure 4) has been more precisely investigated by HRTEM observations and with a higher magnification. Two types of films can be prepared by adjusting the t_{ON} injection time: periodic multilayers or homogeneous tantalum oxide films (Figure 5). For t_{ON} = 3 s (Figure 5a,b), regular and nanometric Ta/TaO_x alternations are clearly produced with a period Λ = 3.4 nm regularly stacked through the total film thickness. The native silicon oxide layer (2–3 nm thick) is also clearly viewed at the film/substrate interface (Figure 5b,d). The highest magnification (Figure 5b) shows that interfaces between metallic Ta (dark bands) and oxide TaO_x (bright bands) sub-layers are not frankly defined but gradually change. Despite very short times of

oxygen gas supplies and stops (a few 10^2 ms are required to stabilize the pulsing signal at the beginning of t_{ON} and t_{OFF} times), oxygen species are not instantaneously evacuated for the sputtering chamber. In addition, oxygen diffusion from TaO_x to Ta sub-layers cannot be neglected leading to gradual and periodic variations of Ta and O concentrations through each sub-layer. However, the profile analysis (to see Figure S1 in Supplementary Materials) clearly brings to the fore the nanometric period with metal and oxide alternations exhibiting a metallic thickness λ_{Ta} = 1.9 nm (dark bands) and an oxide TaO_x sub-layer λ_{TaOx} = 1.5 nm (bright bands). Ta and O atomic concentrations determined by energy-dispersive X-ray spectroscopy reveal an oxygen-rich composition in the oxide sub-layer with 73±4 at. % of O and 27±4 at. % of Ta (to see Figure S2 in Supplementary Materials). These contents correspond to an oxide phase close to the Ta_2O_5 compound. A significant amount of oxygen is measured in metallic sub-layers with 10–19±4 at. % of O and 81–90±4 at. % of Ta, which is assigned to inclusion of oxygen in the Ta sub-layer. Even if a small probe size (1 nm) has been used for the EDX measurements, the presence of oxygen in the metallic sub-layers can also be explained by the widening of the electron beam crossing the specimen.

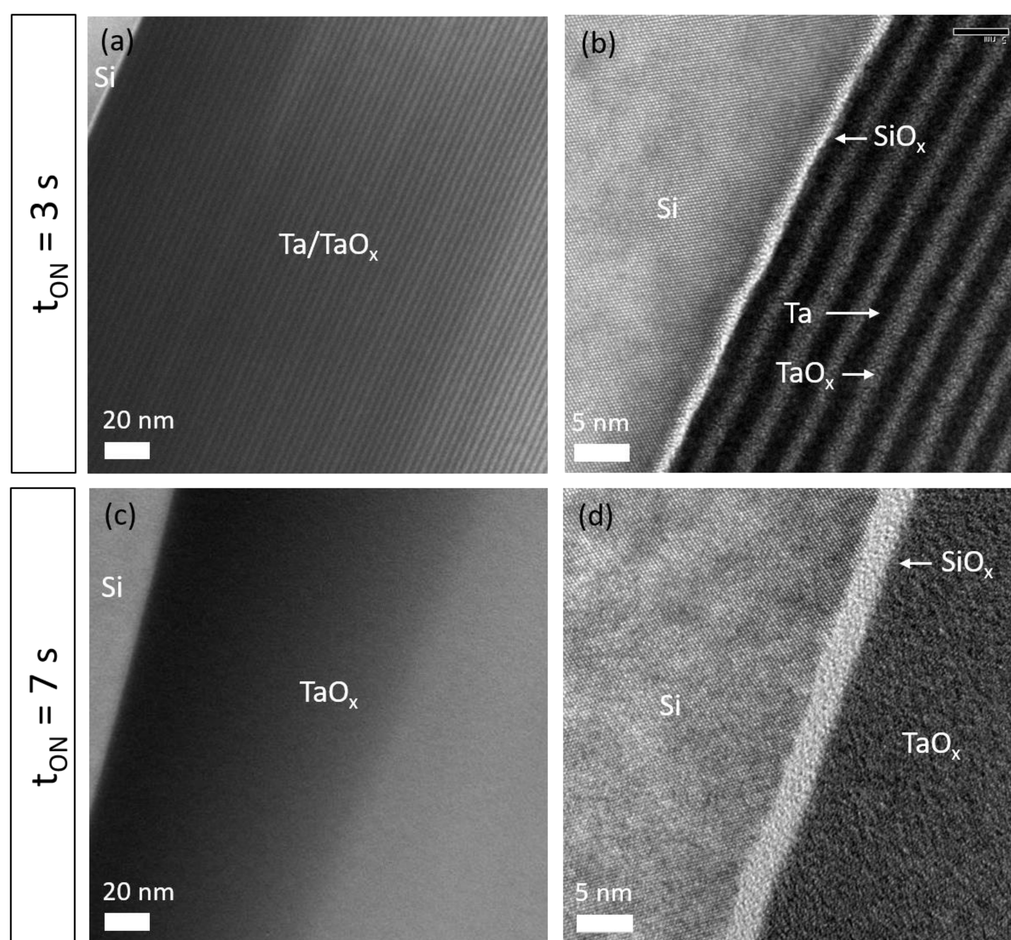

Figure 5. Cross-section views by HRTEM of tantalum oxide thin films sputter-deposited by RGPP using two different t_{ON} injection times: (**a**) and (**b**) t_{ON} = 3 s; (**c**) and (**d**) t_{ON} = 7 s. Periodic Ta/TaO_x multilayers or homogeneous TaO_x films can be prepared by means of a precise and single adjustment of the t_{ON} injection time.

It is also worth of noting that high resolution images and diffraction patterns did not allow to detect any crystalline phase but amorphous Ta and TaO_x sub-layers (to see Figure S3 in Supplementary Materials). A former study focused on Ta/TaO_x multilayers with thicker periods showed that the metallic Ta sub-layer has to be higher than 10 nm to obtain a nanometric crystal of the bcc α-Ta phase; the oxide TaO_x sub-layer remaining amorphous whatever the thickness [45]. In our study, due to the very low thickness of each sub-layer

(lower than 2 nm), one can expect an amorphous structure of Ta and TaO_x alternations. As a result, Ta/TaO_x nanometric multilayers prepared with t_{ON} injection times lower than 5 s are mainly amorphous and can be rather defined as a-Ta:O/a-Ta_2O_5 alternations. For t_{ON} injection times higher than 5 s, homogeneous and amorphous tantalum oxide thin films are obtained (Figure 5c,d). No alternations of bright and dark bands are observed for these pulsing conditions, but a dark grey shading with a random distribution of atoms, as shown in Figure 5d for the highest magnification. Ta and O concentrations are in the range 25–29 ± 4 at. % and 71–75 ± 4 at. %, respectively. These contents agree with the overall composition previously determined by EPMA and presented in Figure 2.

Similar Me/MeO_x, [51] Me/MeN_y, [52] MeN_y/MeO_xN_y [53] periodic multilayers have been reported for other ceramic thin films prepared by reactive sputtering using RGPP but with thicker periods. Other nanocomposite ternary nitrides also showed some attractive improvements of mechanical properties playing with the metal composition, the nanocomposite structure of the multilayered stacking [54,55]. Assuming deposition rates of the pure metal (reactive sputtering process working in elemental mode) and that of the corresponding compound (process in poisoned mode), and if the pulsing period is not too short with a suitable t_{ON} injection time, periodic alternations can be fabricated with a period thickness Λ of a few nanometers and with metal/compound interfaces in the order of the nanometer. However, the smallest metal/compound alternations also depend on the reactivity of the metalloid towards the metal, especially when oxygen is involved with very reactive metals like titanium for instance. For such conditions, no clear multilayers can be reached and kinetics of the reactive sputtering process as well as reactivity of metal vs. metalloid both influence the minimum period thickness and the quality of alternations and interfaces.

3.2. Optical and Electrical Properties

Since tantalum oxide is an attractive thin film material for optical applications, optical transmittance of the films (500 nm thick) deposited on glass substrate has been measured in the visible range and for various t_{ON} injection times (Figure 6).

For films prepared with t_{ON} injection time lower than 5 s, no transmitted signal is measured for wavelengths in between 200 and 1100 nm. Reactive gas supplied in the sputtering process is too short to incorporate enough oxygen in the film. Longer t_{ON} injection times (particularly from 5.3 to 5.8 s) lead to semi-transparent thin films with an optical transmittance of a few %, which progressively increases when the wavelength tends to the infrared region. This range of t_{ON} injection times corresponds to tantalum oxide compounds which are not completely oxidized to form the most stable and stoichiometric Ta_2O_5 material [56]. Some fringes start appearing for $t_{ON} > 5.8$ s but films prepared with such conditions still remains significantly absorbent with an optical transmittance lower than 70% at 1100 nm and gradually diminishing for becoming null at 280 nm. It is worth noting that tantalum and oxygen concentrations remain nearly unchanged (or slightly increase) for t_{ON} injection times in between 5 and 6 s (Figure 2). Despite this, there is very little variation of the film composition; optical transmittance is largely enhanced which is mainly connected to the reduction of oxygen and tantalum defects and vanishing of the periodic multilayer structure as t_{ON} rises.

A further increase in the t_{ON} injection time leads to transparent tantalum oxide thin films (average transmittance higher than 80%) exhibiting typical interferential fringes. It is interesting to observe that from $t_{ON} = 7$ s and when oxygen injection tends to a constant supply, films show nearly the same optical transmittance. This correlates well with a stabilization of the chemical composition (O and Ta concentration become constant, as shown in Figure 2) and a homogeneous structure observed at the nanoscale from HRTEM (Figure 5c,d). The range of t_{ON} injection times included between 5 s and 7 s appears as the most interesting operating conditions to largely tune the optical transmittance of the films from absorbent to transparent in the visible region. In addition, such a range also corresponds to the maximum deposition rate formerly measured and discussed (Figure 1).

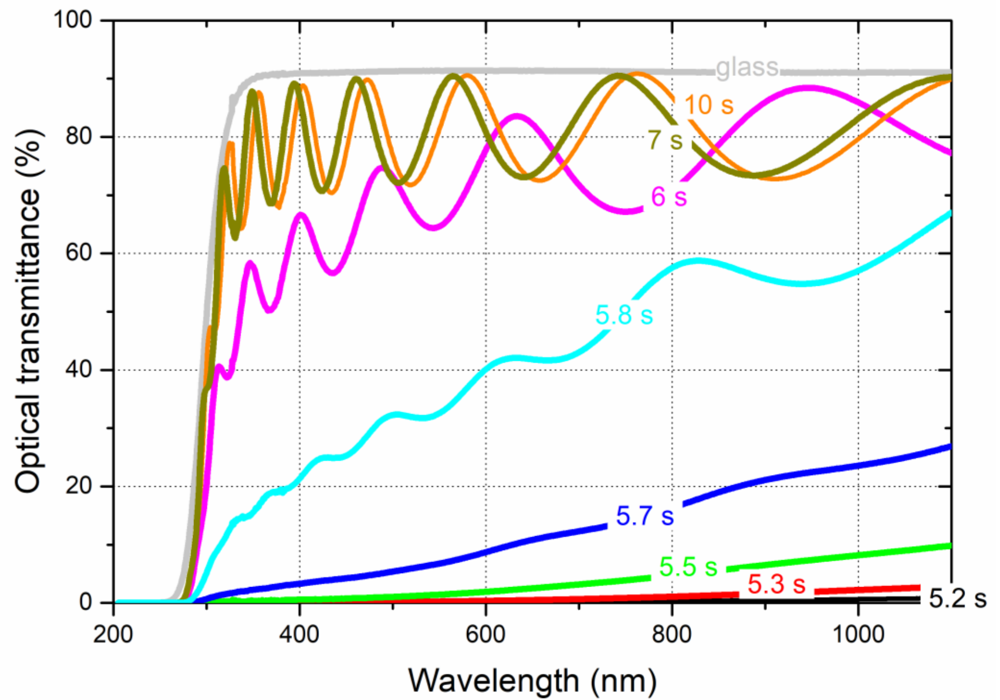

Figure 6. Optical transmittance spectra in the visible range of tantalum oxide thin films sputter-deposited on glass substrate and for different t_{ON} injection times. For t_{ON} lower than 5 s, films are completely absorbent. Glass substrate is also shown as a reference.

Absorption edge in the near UV region is also influenced by the oxygen supply with a blue shift as t_{ON} rises. This behavior has also been measured for other transparent metal oxide films prepared by reactive sputtering likewise pulsing the oxygen gas [57]. It is closely connected to oxygen vacancies in the film, which create states in the optical band gap, below the conduction band [56]. Increasing the t_{ON} injection time until a constant supply of oxygen reduces the density of oxygen deficiency in the films. Optical transparency in the visible region is favored and the band gap increases, which correlates with a slight shift of the absorption edge to lower wavelengths.

This gradual evolution of optical properties corroborates other investigations devoted to some metal oxide thin films prepared by RGPP [58]. Similarly, playing with a suitable range of t_{ON} injection times allows a wide tunability of many physical properties, not solely optical characteristics but electronic transport properties as well. To that end, the electrical conductivity of tantalum oxide thin films prepared on glass substrate and for different t_{ON} injection times was measured as a function of the temperature (Figure 7). Without oxygen injection (t_{ON} = 0 s), conductivity of pure Ta films is higher than 2.06×10^6 S m^{-1} at 300 K and is slightly influenced by the variation of temperature. The evolution of resistivity vs. temperature (not shown here) gives rise to a typical metallic-like behavior with a temperature coefficient of resistance (TCR_{300K}) at a room temperature of 1.16×10^{-3} K^{-1}. This value is lower than that of the bulk (TCR Ta bulk at 300 K is 3.54×10^{-3} K^{-1} [59]) as often reported for thin films and mainly assigned to the number of grain boundaries per electron mean free path in polycrystalline metallic thin films [60]. Increasing such a number, TCR reduces and can even exhibit a change in sign (from positive to negative) although the conductivity is kept in a metallic regime.

Introducing the oxygen gas up to t_{ON} = 4 s leads to more resistive films although the order of magnitude of conductivity is still in the metallic range. Conductivity largely drops to a few 10^5 S m^{-1}, but is inversely influenced by the temperature even for the shortest t_{ON} injection time of 1 s since films become slightly more conductive as the temperature rises. A negative TCR_{300K} is then obtained, which reduces from -2.20×10^{-4} to -2.66×10^{-4} K^{-1} when t_{ON} changes from 1 to 4 s, respectively. This loss of electrical conductivity with a

negative TCR value has been measured for other metal oxide thin films containing a few at. % of oxygen or exhibiting a sub-stoichiometric composition [34,45]. These uncommon electronic transport behaviors are typical of disordered or poorly crystalline metal-rich oxide thin films, especially when Ta β-phase is produced [61]. It is worth noting that this range of t_{ON} injection times corresponds to Ta-rich oxide films (Figure 2), exhibiting a periodic multilayer nanostructure (Figure 5). In addition, films prepared with 1 s ≤ t_{ON} ≤ 4 s are opaque in the visible region (Figure 6) with a poorly crystalline structure composed of α-Ta, β-Ta and amorphous tantalum oxide phase mixture (Figure 3), which finally vanishes to produce a complete amorphous structure for longer t_{ON} injection times.

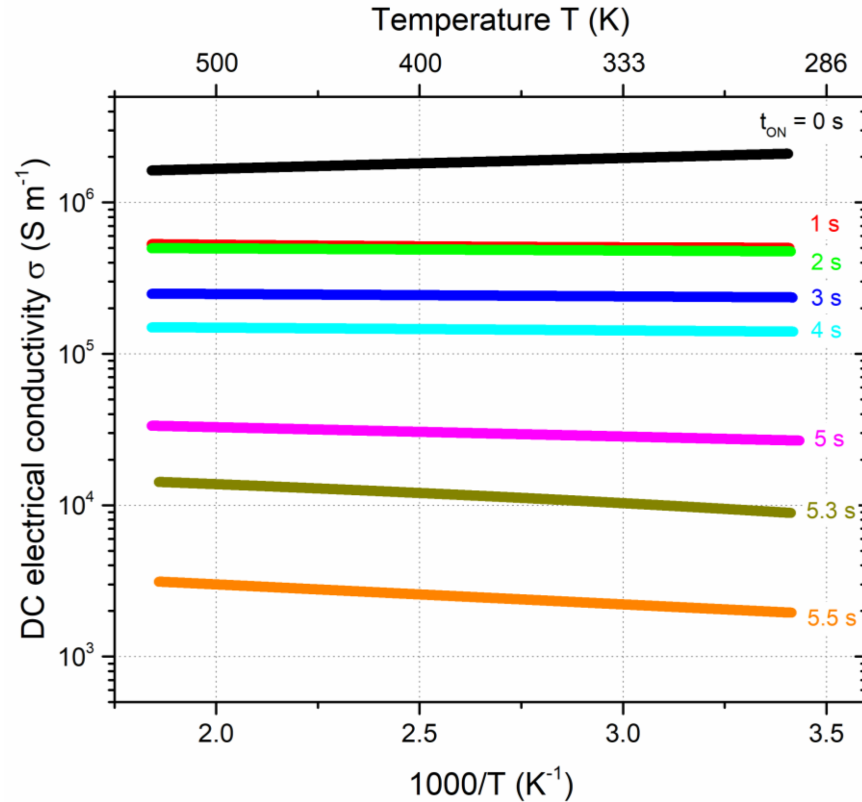

Figure 7. DC electrical conductivity as a function of the reciprocal of temperature 1000/T measured on tantalum oxide films prepared on glass substrate with t_{ON} injection times lower than 5.5 s (the corresponding temperature T is also indicated on the top axis).

Increasing the t_{ON} injection time until a constant oxygen supply produces more resistive films and for t_{ON} higher than 5.5 s, conductivity cannot be measured with our four-probe system. For these deposition conditions, films become semiconductors and lastly insulators. For films obtained with t_{ON} in-between 5 and 5.5 s, conductivity vs. reciprocal temperature (Arrhenius plot) gives rise to a clear linear evolution indicating a thermally activated conduction mechanism. The activation energy calculated for this range of t_{ON} injection times increases from 10 to 26 meV, which are quite low values compared to other oxide materials. These results correlate well with pulsing conditions corresponding to the deposition of oxygen-deficient Ta_2O_5 films. A short increase in the t_{ON} injection time leads to a fast oxygen enrichment of the films and, consequently, they rapidly exhibit dielectric characteristics (transparent in the visible region and insulator). Baker et al. [62] recently reported very similar results on tantalum oxide films prepared by changing the total sputtering pressure in the deposition chamber. They also brought to the fore an abrupt increase in resistivity with an oxygen enrichment of the films. They measured a gradual transition from metallic conduction to an activated tunneling through the oxide phase with an exponential relationship between oxygen concentration and activation energy for films tending to the Ta_2O_5 compound.

4. Conclusions

The 500 nm thick tantalum oxide thin films are sputter-deposited by DC reactive magnetron sputtering. A Ta target is sputtered in a reactive atmosphere composed of Ar and O_2 gases. The Reactive Gas Pulsing Process, namely RGPP, is implemented introducing the oxygen gas with a constant pulsing period T = 10 s while a systematic change in the t_{ON} injection time is performed. A reverse and gradual evolution of tantalum and oxygen concentrations is thus obtained as a function of an increasing t_{ON} injection time leading to an over-stoichiometric Ta_2O_5 compound when the oxygen supply tends to be constant (t_{ON} = T = 10 s). Deposition rate vs. t_{ON} reveals an unusual maximum for intermediate t_{ON} injection times, which is mainly connected to the high sputtering yield of the Ta_2O_5 compound compared to that of the pure Ta metal.

Whatever the oxygen supply, films exhibit a poorly defined columnar morphology with a brittle fracture observed from cross-section views. For the longest t_{ON} injection times, i.e., higher than 5 s, no long-range order is detected but an amorphous structure with a homogeneous and random distribution of atoms. These deposition conditions produce TaO_x films with an adjustable oxygen concentration from sub- to over-stoichiometric Ta_2O_5 compound. Such films also show a transparent optical transmittance in the visible region and thus electrical properties corresponding to semiconducting characteristics with a thermally activated conductivity.

Playing with the t_{ON} injection time in between 1 and 5 s allows the growth of periodic and nanometric Ta/TaO_x multilayers with a regular periodic structure Λ of a few nanometers through the overall film thickness. For these pulsing conditions, both α- and β-Ta phases are obtained with a significant part of an amorphous oxide, which becomes predominant by increasing the t_{ON} injection time. Films exhibit a fully absorbent optical characteristic with a metallic-like electrical behavior. A precise adjustment of the t_{ON} injection time in the range of a few seconds leads to a change in sign (from positive to negative) of the temperature coefficient of resistance although the conductivity is maintained in a metallic regime.

These results clearly demonstrate that pulsing the introduction of the oxygen gas is a powerful tool for producing metal oxide thin films exhibiting a homogeneous or a multilayered structure at the nanoscale with properties ranging from metal to semiconductor and finally insulator playing only with a single deposition parameter: the injection time of the reactive gas. In addition, the experimental approach presented herein can be extended to other types of metal oxide systems or other nitride, carbide, sulfide compounds, and thus to gain insight into growth mechanisms that determine the final nanostructure of films sputter-deposited by RGPP. Last but not least, this reactive gas pulsing strategy can be easily transferred at the industrial scale involving vacuum deposition techniques to produce more complex ceramics such as multinary compounds, with high deposition rates keeping a good control of the reactive sputtering process.

Supplementary Materials:. The following supporting information can be downloaded at: www.mdpi.com/xxx/s1, Figure S1: Intensity profile for a Ta/TaO_x periodic multilayer prepared with an oxygen injection time t_{ON} = 3 s. It has been extracted from a HRTEM image (blue-green area, Figure 5.a) and points out the regular stacked sequence. Lower and higher intensities correspond to metallic and oxide sub-layers, respectively. The background decrease is linked to the variation of the specimen thickness (crossed by the electron beam) after TEM specimen preparation; Figure S2: Typical EDX spectra recorded in a) a Ta sub-layer (Ta: 80 at. %, O: 20 at. %) and b) a TaO_x sub-layer (Ta: 30 at. %, O: 70 at. %). Atomic quantification was performed with the ratio method; Figure S2: Typical diffraction pattern obtained for TaO_x films prepared with t_{ON} injection time higher than 3 s. It confirms the amorphous character of TaO_x, already pointed out by XRD (Figure 3).

Author Contributions: Conceptualization, data curation, writing—review and editing, funding acquisition, N.M.; Methodology, software, formal analysis, validation, J.-M.C.; Writing—review and editing, validation, J.G.; Data curation, writing—review and editing, funding acquisition, V.P. All authors have read and agreed to the published version of the manuscript.

Funding: This research was partially funded by Fonds Européen de Développement Régional—FEDER, grant number CTE 6059 in the framework of the TOOLEXPERT Interreg V project.

Institutional Review Board Statement: Not applicable.

Informed Consent Statement: Not applicable.

Data Availability Statement: All data are presented in the current manuscript.

Acknowledgments: This work has been supported by the Région Bourgogne Franche-Comté and by EIPHI Graduate School (Contract 'ANR-17-EURE-0002').

Conflicts of Interest: The authors declare no conflicts of interest. The funders had no role in the design of the study; in the collection, analyses, or interpretation of data; in the writing of the manuscript; or in the decision to publish the results.

References

1. Kim, H.J.; Park, K.; Kim, H.J. High-performance vacuum-processes metal oxide thin-film transistors: A review of recent developments. *J. Soc. Inf. Disp.* **2020**, *28*, 591–622. https://doi.org/10.1002/jsid.886.
2. Chen, R.; Lan, L. Solution-processed metal-oxide thin-film transistors: A review of recent developments. *Nanotechnol*ogy **2019**, *30*, 312001. https://doi.org/10.1088/1361-6528/ab1860.
3. Barsan, N.; Koziej, D.; Weimar, U. Metal oxide-based gas sensor research: How to? *Sens. Actuators B Chem.* **2007**, *121*, 18–35. https://doi.org/10.1016/j.snb.2006.09.047.
4. Granqvist, C.G. Transparent conductive electrodes for electrochromic devices: A review. *Appl. Phys. A* **1993**, *57*, 19–24. https://doi.org/10.1007/bf00331211.
5. Kim, J.S.; Kim, B.; Kim, H.; Kang, K. Recent progress on multimetal oxide catalysts for the oxygen evolution reaction. *Adv. Energy Mater.* **2018**, *8*, 1702774. https://doi.org/10.1002/aenm.201702774.
6. Losego, M.D.; Efremenko, A.Y.; Rhodes, C.L.; Cerruti, M.G.; Franzen, S.; Maria, J.P. Conductive oxide thin films: Model systems for understanding and controlling surface plasmon resonance. *J. Appl. Phys.* **2009**, *106*, 024903. https://doi.org/10.1063/1.3174440.
7. Chittinan, D.; Buranasiri, P.; Lertvanithphol, T.; Eiamchai, P.; Tantiwanichapan, K.; Sathukarn, A.; Limwichean, S.; Klamchuen, A.; Wutikhun, T.; Limsuwan, P.; et al. Tailoring the structural and optical properties of fabricated TiO_2 thin films by O_2 duty cycle in reactive gas-timing magnetron sputtering. *Vacuum* **2023**, *214*, 112205. https://doi.org/10.1016/j.vacuum.2023.112205.
8. Medvedeva, J.E.; Buchholz, D.B.; Chang, R.P.H. Recent advances in understanding the structure and properties of amorphous oxide semiconductors. *Adv. Electron. Mater.* **2017**, *3*, 1700082. https://doi.org/10.1002/aelm.201700082.
9. Moreira, H.; Costa-Barbosa, A.; Mariana Marques, S.; Sampaio, P.; Carvalho, S. Evaluation of cell activation promoted by tantalum and tantalum oxide coatings deposited by reactive DC magnetron sputtering. *Surf. Coat. Technol.* **2017**, *330*, 260–269. https://doi.org/10.1016/j.surfcoat.2017.10.019.
10. Sharath, S.U.; Joseph, M.J.; Vogel, S.; Hildebrandt, E.; Komissinskiy, P.; Kurian, J.; Schroeder, T.; Alff, L. Impact of oxygen stoichiometry on electroforming and multiple switching modes in TiN/TaO_x/Pt based ReRAM. *Appl. Phys. Lett.* **2016**, *109*, 173503. https://doi.org/10.1063/1.4965872.
11. Franke, E.; Schubert, M.; Trimble, C.L.; Devries, M.J.; Woollam, J.A. Optical properties of amorphous and polycrystalline tantalum oxide measured by spectroscopic ellipsometry. *Thin Solid Film.* **2001**, *388*, 283–289. https://doi.org/10.1016/s0040-6090(00)01881-2.
12. Kazuki, T.; Yasusei, Y.; Shanhu, B.; Masahisa, O.; Kazuki, Y. Solid electrolyte of tantalum oxide thin film deposited by reactive DC and RF magnetron sputtering for all-solid-state switchable mirror glass. *Sol. Energy Mater. Sol. Cells* **2008**, *92*, 120–125. https://doi.org/10.1016/j.solmat.2007.01.022.
13. Borisenko, V.E.; Parkhutik, V.P. RBS study of transient thermal anodic oxidation of tantalum films. *Phys. Status Solidi A Appl. Mat.* **1986**, *93*, 123–130. https://doi.org/10.1002/pssa.2210930116.
14. Gangloff, D.; Shi, M.; Wu, T.; Bylinskii, A.; Braverman, B.; Gutierrez, M.; Nichols, R.; Li, J.; Aichholz, K.; Cetina, M.; et al. Preventing and reversing vacuum-induced optical losses in high-finesse tantalum (V) oxide mirror coatings. *Opt. Express* **2015**, *23*, 18014–18028. https://doi.org/10.1364/oe.23.018014.
15. Yun, S.N.; Wang, L.; Guo, W.; Ma, T.L. Non-Pt counter electrode catalysts using tantalum oxide for low-cost dye-sensitized solar cells. *Electrochem. Commun.* **2012**, *24*, 69–73. https://doi.org/10.1016/j.elecom.2012.08.008.
16. Schmitt, K.; Oehse, K.; Sulz, G.; Hoffmann, C. Evanescent field sensors based on tantalum pentoxide waveguides—A review. *Sensors* **2007**, *8*, 711–738. https://doi.org/10.3390/s8020711.
17. Rouahi, A.; Challali, F.; Dakhlaoui, I.; Vallee, C.; Salimy, S.; Jomni, F.; Yangui, B.; Besland, M.P.; Goullet, A.; Sylvestre, A. Structural and dielectric characterization of sputtered tantalum titanium oxide thin films for high temperature capacitor applications. *Thin Solid Film.* **2016**, *606*, 127–132. https://doi.org/10.1016/j.tsf.2016.03.047.
18. Kimura, H.; Mizuki, K.; Kamiyama, S.; Suzuki, H. Extended X-ray absorption fine-structure analysis of the difference in local-structure of tantalum oxide capacitor films produced by various annealing methods. *Appl. Phys. Lett.* **1995**, *66*, 2209–2221. https://doi.org/10.1063/1.113169.
19. Lau, W.S.; Tan, T.S.; Babu, P.; Sandler, N.P. Mechanism of leakage current reduction of tantalum oxide capacitors by titanium doping. *Appl. Phys. Lett.* **2007**, *90*, 112903. https://doi.org/10.1063/1.2710000.

20. Yu, H.B.; Zhu, S.Y.; Yang, X.; Wang, X.H.; Sun, H.W.; Huo, M.X. Synthesis of coral-like tantalum oxide films via anodization in mixed organic-inorganic electrolytes. *PLoS ONE* **2013**, *8*, e66447. https://doi.org/10.1371/journal.pone.0066447.
21. Ohno, T.; Samukawa, S. Resistive switching in a few nanometers thick tantalum oxide thin film formed by a metal oxidation. *Appl. Phys. Lett.* **2015**, *106*, 173110. https://doi.org/10.1063/1.4919724.
22. He, X.M.; Wu, J.H.; Zhao, L.L.; Mang, J.; Gao, X.D.; Li, X.M. Synthesis and optical properties of tantalum oxide films prepared by ionized plasma-assisted pulsed laser deposition. *Solid State Commun.* **2008**, *147*, 90–93. https://doi.org/10.1016/j.ssc.2008.05.007.
23. Kim, I.; Ahn, S.D.; Cho, B.W.; Ahn, S.T.; Lee, J.Y.; Chun, J.S.; Lee, W.J. Microstructure and electrical properties of tantalum oxide thin film prepared by electron cyclotron resonance plasma enhanced chemical vapor deposition. *Jpn. J. Appl. Phys.* **1994**, *33*, 6691–6698. https://doi.org/10.1143/jjap.33.6691.
24. Rahmati, B.; Sarhan, A.A.D.; Zalnezhad, E.; Kamiab, Z.; Dabbagh, A.; Choudhury, D.; Abas, W.A.B.W. Development of tantalum oxide (Ta-O) thin film coating on biomedical Ti-6Al-4V alloy to enhance mechanical properties and biocompatibility. *Ceram. Int.* **2016**, *42*, 466–480. https://doi.org/10.1016/j.ceramint.2015.08.133.
25. Wang, S.C.; Liu, K.Y.; Huang, J.L. Tantalum oxide film prepared by reactive magnetron sputtering deposition for all-solid-state electrochromic device. *Thin Solid Film.* **2011**, *520*, 1454–1459. https://doi.org/10.1016/j.tsf.2011.08.046.
26. Ngaruiya, J.M.; Venkataraj, S.; Drese, R.; Kappertz, O.; Leervad Pedersen, T.; Wuttig, M. Preparation and characterization of tantalum oxide films produced by reactive DC magnetron sputtering. *Phys. Status Solidi* **2003**, *198*, 99–110. https://doi.org/10.1002/pssa.200306444.
27. Depla, D.; De Gryse, R. Target poisoning during reactive magnetron sputtering: Part I: The influence of ion implantation. *Surf. Coat. Technol.* **2004**, *183*, 184–189. https://doi.org/10.1016/j.surfcoat.2003.10.006.
28. Berg, S.; Särhammar, E.; Nyberg, T. Upgrading the "Berg-model" for reactive sputtering processes. *Thin Solid Film.* **2014**, *565*, 186–192. https://doi.org/10.1016/j.tsf.2014.02.063.
29. Billard, A.; Frantz, C. Attempted modelling of thickness and chemical heterogeneity in coatings prepared by dc reactive magnetron sputtering. *Surf. Coat. Technol.* **1993**, *59*, 41–47. https://doi.org/10.1016/0257-8972(93)90052-p.
30. Martin, N.; Lintymer, J.; Gavoille, J.; Chappé, J.M.; Sthal, F.; Takadoum, J.; Vaz, F.; Rebouta, L. Reactive sputtering of TiO_xN_y coatings by the reactive gas pulsing process—Part II : The role of the duty cycle. *Surf. Coat. Technol.* **2007**, *201*, 7727–7732. https://doi.org/10.1016/j.surfcoat.2007.03.021.
31. Petitjean, C.; Rousselot, C.; Pierson, J.F.; Billard, A. Reactive sputtering of iron in Ar-N_2 and Ar-O_2 mixtures. *Surf. Coat. Technol.* **2005**, *200*, 431–434. https://doi.org/10.1016/j.surfcoat.2005.02.028.
32. Depla, D.; Haemers, J.; De Gryse, R. Discharge voltage measurements during reactive sputtering of oxides. *Thin Solid Film.* **2006**, *515*, 468–471. https://doi.org/10.1016/j.tsf.2005.12.256.
33. Khemasiri, N.; Chananonnawathorn, C.; Klamchuen, A.; Jessadaluk, S.; Pankiew, A.; Vuttivong, S.; Eiamchai, P.; Horprathum, M.; Pornthreeraphat, S.; Kasamechonchung, P.; et al. Crucial role of reactive pulse-gas on a sputtered Zn_3N_2 thin film formation. *RSC Adv.* **2016**, *6*, 94905–94910. https://doi.org/10.1039/c6ra09972f.
34. Xu, X.; Yazdi, M.A.P.; Salut, R.; Cote, J.M.; Billard, A.; Martin, N. Structure, composition and electronic transport properties of tungsten oxide thin films sputter-deposited by the reactive gas pulsing process. *Mater. Chem. Phys.* **2018**, *205*, 391–400. https://doi.org/10.1016/j.matchemphys.2017.11.048.
35. Oechsner, H.; Schoof, H.; Stumpe, E. Sputtering of Ta_2O_5 by Ar^+ ions at energies below 1 keV. *Surf. Sci.* **1978**, *76*, 343–354. https://doi.org/10.1016/0039-6028(78)90102-4.
36. Djeffal, F.; Martin, N.; Ferhati, H.; Benhaya, A. Tunable band-selective photodetector based on sputter-deposited SnO_x thin-films: Effect of reactive gas pulsing process. *J. Alloys Compd.* **2023**, *968*, 171851. https://doi.org/10.1016/j.jallcom.2023.171851.
37. Sproul, W.D. High-rate reactive sputtering process-control. *Surf. Coat. Technol.* **1987**, *33*, 73–81. https://doi.org/10.1016/0257-8972(87)90178-2.
38. Hmiel, A.F. Partial-pressure control of reactively sputtered titanium nitride. *J. Vac. Sci. Technol.* **1985**, *A3*, 592–595. https://doi.org/10.1116/1.572957.
39. Larsson, T.; Blom, H.O.; Nender, C.; Berg, S. A physical model for eliminating instabilities in reactive sputtering. *J. Vac. Sci. Technol.* **1988**, *A6*, 1832–1836. https://doi.org/10.1116/1.575264.
40. Baker, P.N. Preparation and properties of tantalum thin films. *Thin Solid Film.* **1972**, *14*, 3–25. https://doi.org/10.1016/0040-6090(72)90365-3.
41. Knepper, R.; Stevens, B.; Baker, S.P. Effect of oxygen on the thermomechanical behavior of tantalum thin films during the β-α phase formation. *J. App. Phys.* **2006**, *100*, 123508. https://doi.org/10.1063/1.2388742.
42. Feinstein, L.G.; Huttemann, R.D. Factors controlling the structure of sputtered Ta films. *Thin Solid Film.* **1973**, *16*, 129–145. https://doi.org/10.1016/0040-6090(73)90163-6.
43. Garg, S.P.; Krishnamurty, N.; Awasthi, A.; Venkatraman, M. The Ta-O (Oxygen-Tantalum) system. *J. Phase Equilibria* **1996**, *17*, 63–77. https://doi.org/10.1007/bf02648373.
44. Colin, J.J.; Abadias, G.; Michel, A.; Jaouen, C. On the origin of the metastable β-Ta phase in tantalum sputtered thin films. *Acta Mater.* **2017**, *126*, 481–493. https://doi.org/10.1016/j.actamat.2016.12.030.
45. Cacucci, A.; Loffredo, S.; Potin, V.; Imhoff, L.; Martin, N. Interdependence of structural and electrical properties in tantalum/tantalum oxide multilayers. *Surf. Coat. Technol.* **2013**, *227*, 38–41. https://doi.org/10.1016/j.surfcoat.2012.10.064.
46. Zhou, J.C.; Luo, D.T.; Li, Y.Z.; Liu, Z. Effect of sputtering pressure and rapid thermal annealing on optical properties of Ta_2O_5 thin films. *Trans. Nonferrous Met. Soc. China* **2009**, *19*, 359–363. https://doi.org/10.1016/s1003-6326(08)60278-2.

47. Vlcek, J.; Rezek, J.; Houska, J.; Cerstvy, R.; Bugyi, R. Process stabilization and a significant enhancement of the deposition rate in reactive high-power impulse magnetron sputtering of ZrO_2 and Ta_2O_5 films. *Surf. Coat. Technol.* **2013**, *236*, 550–556. https://doi.org/10.1016/j.surfcoat.2013.10.052.
48. Chittinan, D.; Buranasiri, P.; Lertvanithphol, T.; Eiamchai, P.; Patthanasettakul, V.; Chananonnawathorn, C.; Limwichean, S.; Nuntawong, N.; Klamchuen, A.; Muthitamongkol, P.; et al. Observations of the initial stage on reactive gas-timing sputtered TaO thin films by dynamic in situ spectroscopic ellipsometry. *Optic. Mater.* **2019**, *92*, 223–232. https://doi.org/10.1016/j.optmat.2019.04.040.
49. Ito, Y.; Abe, Y.; Kawamura, M.; Kim, K.H.; Kiba, T. Influence of substrate cooling on ion conductivity of tantalum oxide thin films prepared by reactive sputtering using water vapor injection. *Thin Solid Film.* **2020**, *710*, 138276. https://doi.org/10.1016/j.tsf.2020.138276.
50. Thornton, J.A. Influence of apparatus geometry and deposition conditions on the structure and topography of thick sputtered coatings. *J. Vac. Sci. Technol.* **1974**, *11*, 666–670. https://doi.org/10.1116/1.1312732.
51. Parreira, N.; Polcar, T.; Cavaleiro, A. Characterization of W-O coatings deposited by magnetron sputtering with reactive gas pulsing. *Surf. Coat. Technol.* **2007**, *201*, 5481–5486. https://doi.org/10.1016/j.surfcoat.2006.07.017.
52. El Mouatassim, A.; Pac, M.J.; Pailloux, F.; Amiard, G.; Henry, P.; Rousselot, C.; Eyidi, D.; Tuilier, M.H.; Cabioc'h, T. On the possibility of synthesizing multilayered coatings in the (Ti, Al)N system by RGPP: A microstructural study. *Surf . Coat. Technol.* **2019**, *374*, 845–851. https://doi.org/10.1016/j.surfcoat.2019.06.071.
53. Fenker, M.; Kappl, H.; Sandu, C.S. Precise control of multilayered structures of Nb-O-N thin films by the use of reactive gas pulsing process in DC magnetron sputtering. *Surf. Coat. Technol.* **2008**, *202*, 2358–2362. https://doi.org/10.1016/j.surfcoat.2007.08.007.
54. Sahu, B.P.; Ray, M.; Mitra, R. Structure and properties of $Ni_{1-x}Ti_xN$ films processed by reactive magnetron co-sputtering. *Mater. Charact.* **2020**, *169*, 110604. https://doi.org/10.1016/j.matchar.2020.110604.
55. Moganapriya, C.; Rajasekar, R.; Ponappa, K.; Karthick, R.; Perundurai, R.V.; Kumar, P.S.; Pal, S.K. Tribomechanical behavior of TiCN/TiAlN/WC-C multilayer film on cutting tool inserts for machining. *Mater. Test.* **2017**, *59*, 703–707. https://doi.org/10.3139/120.111060.
56. Li, J.; Liu, W.; Wei, Y.; Yan, Y. Effect of oxygen content on the properties of sputtered TaOx electrolyte film in all-solid-state electrochromic devices. *Coatings* **2022**, *12*, 1831. https://doi.org/10.3390/coatings12121831.
57. Springer, S.G.; Schmid, P.E.; Sanjinès, R.; Lévy, F. Morphology and electrical properties of titanium oxide nanometric multilayers deposited by DC reactive sputtering. *Surf. Coat. Technol.* **2002**, *151–152*, 51–54. https://doi.org/10.1016/s0257-8972(01)01584-5.
58. Martin, N.; Besnard, A.; Sthal, F.; Takadoum, J. The reactive gas pulsing process for tuneable properties of sputter deposited titanium oxide, nitride and oxynitride coatings. *Inter. J. Mater. Prod. Technol.* **2010**, *39*, 159–177. https://doi.org/10.1504/ijmpt.2010.034268.
59. Desal, P.D.; Chu, T.K.; James, H.M.; Ho, C.Y. Electrical resistivity of selected elements. *J. Phys. Chem. Ref. Data* **1984**, *13*, 1069–1096. https://doi.org/10.1063/1.555723.
60. Reiss, G.; Vancea, J.; Hoffman, H. Grain-boundary resistance in polycrystalline metals. *Phys. Rev. Lett.* **1986**, *56*, 2100–2103. https://doi.org/10.1103/physrevlett.56.2100.
61. Schwartz, N.; Reed, W.A.; Polash, P.; Read, M.H. Temperature coefficient of resistance of beta-tantalum films and mixtures with b.c.c.-tantalum. *Thin Solid Film.* **1972**, *14*, 333–347. https://doi.org/10.1016/0040-6090(72)90433-6.
62. Baker, A.; Engwall, A.M.; Bayu-Aji, L.B.; Bae, J.H.; Shin, S.J.; Moody, J.D.; Kucheyev, S.O. Tantalum suboxide films with tunable composition and electrical resistivity deposited by reactive magnetron sputtering. *Coatings* **2022**, *12*, 917. https://doi.org/10.3390/coatings12070917.